Human NK cells engage cell-intrinsic non-canonical inflammasome function

Nathan G.F. Leborgne[1,3], Jadie Acklam[1,3,5], Alexander J. Hogg[1,3,5],Zarema Albakova[1,3], Karen G. Hogg[1], Kim Samirah Robinson[1,2], Grant Calder[1], Arnel Villamin Jr[1,3], Callum Robson,[1,3], Freya Pealing[1,3] ,Matthew A. Care[1,3], Monika Gonka[1,3], James M. Fox[1], James Iremonger[4], Frances E. Pearson[4], Max E. Noble[4] , Alison M. Layton[2], James P. Hewitson[1,3,5], David G. Kent[1,3,5], , William Grey[1,3], Jillian L. Barlow[1,3,6], Dave Boucher[1,3,6,7]

1 York Biomedical Research Institute, University of York, Biology Department, Wentworth Way, York, YO10 5DD
2 Hull York Medical School, University of York, York, United Kingdom
3 Center for Blood Research
4 VISFO, The Old Flour Mill, Mill Royd Street, Brighouse, West Yorkshire, HD6 1EY
5 These authors contributed equally
6 Senior Author
7 Lead contact: Correspondence to dave.boucher@york.ac.uk

Short Title: A specialised inflammasome in human Natural Killer cells

Abstract

Inflammasome pathways are critical for detecting pathogens and initiating inflammatory responses, yet how individual cell types configure these signalling platforms remains poorly understood. Here, we demonstrate that human Natural Killer cells possess distinct inflammasome machinery, lacking canonical components and innate sensors (NLRP3, NLRC4, TLR4) but harbour a functional non-canonical inflammasome (NCI). Using *Salmonella* enterica Typhimurium infection of primary human NK cells, we show that cytosolic bacterial access triggers caspase-4-dependent pyroptosis and IL-18 secretion, without canonical inflammasome activation or IL-1β production. Strikingly, murine NK cells express inflammasome transcripts but lack functional caspase-11 protein and do not undergo pyroptosis upon infection, revealing species-specific post-transcriptional regulation. We further identify IL-12, but not IFNγ, as a priming signal for NCI components in human NK cells, a functional distinction from macrophages and epithelial cells. Together, these findings reveal that human NK cells have evolved a specialised inflammasome with unique regulatory inputs, establishing these cells as autonomous sensors of intracellular Gram-negative infection.

156 words

Introduction

Innate immune responses are controlled by cellular pathways that coordinate immunity to rapidly eliminate pathogens and restore homeostasis (1). Inflammasomes are critical signalling platforms controlling responses to sterile and infectious agents in immune and epithelial cells (2,3). The inflammasome pathway senses triggers using pattern-recognition receptors (PRRs), which include members of the Nod-like Receptor family (Nod-like receptor protein-1, NLRP1, and -3, NLRP3) and the NLR family CARD domain-containing protein 4 (NLRC4) (2). Unlike the canonical inflammasome, which activates caspase-1 upon detection of bacterial ligands (*e.g.,* flagellin), and self-derived danger signals (*e.g.,* ATP, nucleic acids), the non-canonical inflammasome (NCI) activates caspase-4 and caspase-5 (humans) and caspase-11 (mice) upon recognition of cytosolic bacterial lipopolysaccharides (LPS) (4–6) or from intracellular delivery of outer membrane vesicles (7). In non-phagocytic cells, such as epithelial cells, LPS is presented to caspase-4 through interferon-inducible proteins called guanylate-binding proteins (GBPs) (8–12). GBP1 is a direct LPS sensor and is involved in NCI activation in human cells upon *Salmonella* infection (9,12). NCI signalling leads to the maturation and secretion of pro-inflammatory cytokines (13) and to pyroptosis, a form of pro-inflammatory cell death (14). Pyroptosis is driven by the caspase-mediated cleavage of the pore-forming protein Gasdermin D (GSDMD) (14–16), which activates a Ninjurin-1 (NINJ1)-dependent plasma membrane rupture (17), and is critical to control infections, limiting their spread and mobilising further immune cells for pathogen clearance (18). Pyroptosis mediates the release of antigens, which support adaptive responses (19). Additionally, GSDMD pores mediate potassium influx, which activates the NLRP3 canonical inflammasome downstream of caspase-4/11 (20–22). Inflammasome activation in macrophages and epithelial cells induces the maturation and secretion of interleukin-18 (IL-18) and IL-1β, which are released through the GSDMD pores (23,24). These cytokines generate antimicrobial responses in myeloid, lymphoid, and epithelial cells (25).

Discovered in the 1970s, NK cells are part of the now-expanded family of innate lymphoid cells (ILCs), including ILC1s, ILC2s, ILC3s, and lymphoid tissue-inducer cells. They play key roles in viral and tumour responses and are increasingly studied *ex vivo* as part of novel immunotherapy against cancer (26,27). Functionally, these cells are broadly divided into cytotoxic NK cells (release of perforin, granzyme and defined as $CD56^{dim}CD16^{+}$) and immunoregulatory NK cells (IL-12- and IL-18-

dependent release of proinflammatory cytokines, IFNγ, CCL3, GM-CSF and defined as $CD56^{high}CD16^{low}$) (28,29). Progress has been made in recent years on the contribution of NK cells to early responses during microbial infection. Several studies have shown that NK cells indirectly respond to bacterial infection via IL-12 and IL-18 secreted by accessory cells such as macrophages and dendritic cells, leading to IFN-γ production. (30–32). Human NK cells can also directly recognise bacterial PAMPs, such as outer membrane protein A (OmpA), flagellin, and bacillus Calmette-Guérin (BCG), via TLR2, TLR5, or NKp44, respectively, triggering NK proliferation, IFN-γ production, and α-defensin release without requiring accessory cells (33,34). However, our knowledge of direct bacterial recognition by NK cells remains limited.

Inflammasomes influence adaptive responses in NK, B, and T cells through cytokine-driven and pyroptosis-mediated antigen release from myeloid and epithelial cells (19). As such, inflammasomes are an important part of strong immune responses to vaccines and long-term defence against pathogens (35,36). Recently, cell-intrinsic inflammasome-dependent pyroptosis was demonstrated in naive T cells (37,38). Moreover, it is now established that inflammasome derived-IL-18 can activate NK cells and promote the expression of interferon-γ (IFNγ) and cytotoxic effectors (39). Thus, NK cells are currently viewed as a downstream effector in the inflammasome pathway.

To date, inflammasome functions have mainly been studied in myeloid and epithelial cells where Gram-negative bacteria, such as *Salmonella*, are detected through exposure to a range of Pathogen-Associated Molecular Patterns (PAMPs), including type III secretion system components, flagellin and LPS (40,41). Whether NK cells possess effector and cell-intrinsic inflammasome activity has not been investigated.

Here, we investigate how inflammasomes shape NK cell behaviours during infection with the Gram-negative bacteria *Salmonella enterica* Typhimurium. Using primary human NK cells isolated from blood, we identified a unique inflammasome signature that drives NCI activation but not canonical inflammasome activation. This signature was further enhanced upon IL-12 priming and was absent in mouse NK cells. Our findings highlight the unique regulation and roles of the inflammasome in human NK cells and describe direct intracellular sensing functions during gram-negative infections.

106 **Results**

107

108 **Human NK cells possess a functional non-canonical inflammasome**

109

110 We took advantage of a substantial dataset of healthy human blood NK cells to
111 profile the expression of inflammasome pathway components in these cells where
112 gene and protein expression data in human blood NK cells from 13 healthy donors
113 (36,270 high-quality filtered cells) were grouped functionally as, NK1 ($CD56^{dim}$
114 $CD16^{high}CD3^{-}CD127^{-}CD57^{-}CD2^{-}$, further divided as subtype A, B, and C), NK2
115 ($CD56^{high}CD16^{-}CD3^{-}CD127^{+}CD57^{-}$ $CD2^{+}$), NK3 ($CD56^{dim}CD16^{high}CD3^{-}CD127^{-}$
116 $CD57^{+}CD2^{-}$), and NKint (42). As expected, *GZMB, GZMA,* and *PRF1 showed* higher
117 mean expression in NK1 and NK3 cells (**Figure 1A**). Strikingly, canonical
118 inflammasome components (*NLRP3*, *NLRC4*), the pro-inflammatory cytokine IL-1β,
119 and the receptor detecting extracellular LPS (*TLR4*), were not expressed (40,43,44).
120 *CASP1* and *GSDMD* were detected in NK1 and NK3, but not in NK2 subtype.
121 However, we were able to observe increased mean expression of NCI components,
122 including *CASP4*, *GBP1*, and *GBP2*, in NK1 and NK3 cells, compared to NK2 cells.
123 Other inflammasome-related genes were further restricted, with *GBP4* expressed only
124 in NK1B and NK2, and *PYCARD* in NK1B and NK1C (**Figure 1A**). To exclude the
125 possibility that this was blood-specific, we examined gene expression in human foetal
126 thymic (tissue-resident) NK cells and confirmed that *NLRP3*, *NLRC4*, and *TLR4* were
127 not expressed. We identified a $CASP4^{+}GBP2^{+}$ NK cell population, in which *CASP1,*
128 *GSDMD*, and *PRF1* were upregulated in cycling cells, as compared to non-cycling
129 cells (**Supp. Figure 1A**). This suggests the ability of specific NK cell populations to
130 respond to intracellular Gram-negative infections in different tissues.

131 To confirm the findings from these datasets, we next isolated human peripheral
132 blood NK cells and neutrophils, paired from the same donor and performed
133 quantitative PCR for inflammasome-related genes. Alongside GZMA expression, NK
134 cells also showed low expression of *CASP1*, *CASP4*, and *GSDMD*, with greater
135 expression of *GBP2* (**Figure 1B**). This was compared to expression of these genes in
136 neutrophils, but whilst neutrophils showed gene expression for *TLR4* and *NLRP3,* NK
137 cells did not (**Figure 1C and Supp. Figure 1B**). Analysis of human blood NK cells,
138 using macrophages as a comparison, by western blot also indicated lower protein
139 expression of caspase-1, caspase-4, and GBP1 in NK cells, and similar levels of GBP2

140 and GBP5. We identified NK-specific proteoforms of GBP1 and GBP5 (**Figure 1D**),
141 also previously reported in HUVEC cells (45). Overall, these data reveal that human
142 NK cells operate a minimalist inflammasome system, lacking the canonical machinery
143 (NLRP3, NLRC4, TLR4) that defines macrophage responses to *Salmonella*. Instead,
144 this suggests they rely exclusively on the NCI pathway for bacterial detection.

145 To test the activation of the NCI in the context of infection, we next expanded
146 negatively-selected human peripheral blood NK cells *in vitro* for 14 days, resulting in
147 a highly enriched population containing all NK cell subpopulations, as compared to NK
148 cells directly isolated from fresh blood (**Supp. Figure 2**). We infected the NK cells with
149 *Salmonella enterica* Typhimurium, strain SL1344 and LT2, which infect cell types such
150 as macrophages and epithelial cells, activating canonical (NLRP3, NLRC4; caspase-
151 1) and non-canonical (GBPs; caspase-4,-5) inflammasomes. Infection resulted in a
152 statistically significant increase in lytic cell death, as measured by LDH release (**Figure**
153 **2A**), compared to uninfected cells. This cell death was decreased with the addition of
154 the caspase-1/-4 inhibitor, VX-765 (46) (**Figure 2A**) and upon infection with *SalΔorgA,*
155 a *Salmonella* mutant lacking the functional SPI1 injectisome required for the invasion
156 of non-phagocytic cells (47) (**Figure 2B**). Indeed, *Salmonella* enter the cytosol (9,10)
157 by using a subset of effectors (48), including the needle injectisome protein, OrgA,
158 where its deletion strongly reduces *Salmonella* invasion of non-phagocytic cells (40).
159 Thus, our data not only suggest a caspase-1/-4-dependent cell death mechanism, but
160 also that NK cell lytic death requires intracellular *Salmonella* invasion.

161 Central to the activation of the NCI is the maturation and secretion of pro-
162 inflammatory cytokines, such as IL-1β and IL-18. Our data confirm that priming with
163 LPS or IFNγ, or infection with *S.* Typhimurium induces IL-1β gene expression (**Figure**
164 **2C**) and its secretion (**Figure 2D**) in human neutrophils and macrophages. However,
165 IL-1β was not detectable in NK cells under the same conditions in matched donors.
166 Strikingly, *S.* Typhimurium infection of NK cells induced a statistically significant
167 increase in IL-18 production, which was caspase-1/-4-dependent (**Figure 2E**).

168 As *Salmonella* has been shown to activate multiple inflammasomes during
169 infection, we investigated the pathways involved in such a response. Interestingly, we
170 could not detect the cleaved caspase-1 fragments (p20/p10) upon *Salmonella*
171 infection (**Figure 2F**). Additionally, Nigericin treatment induced an NLRP3-
172 independent cell death in NK cells, as shown with the addition of its inhibitor, MCC950

173 (49) (**Supp. Figure 3A**). NLRP3-dependent caspase-1 cleavage was also not
174 observed in NK cells (**Supp. Figure 3B**). Moreover, Val-boroPro (VbP, NLRP1
175 inflammasome activator, (50)) did not lead to GSDMD cleavage in NK cells but was
176 observed in a keratinocyte cell line (N/TERT) (**Supp. Figure 3C - D**)
177 Our data suggest a distinct mechanism of *Salmonella* sensing in NK cells that
178 does not involve canonical inflammasome signalling, as evidenced by the
179 undetectable gene expression level of NLRC4 and NLRP3 and the absence of
180 response to NLRP3 and NLRP1 triggers. Instead, NK cells utilise a pathway that leads
181 to inflammatory caspase-dependent pyroptosis, and IL-18 secretion, but not IL-1β. In
182 addition, the absence of *TLR4* expression in NK cells, which has been shown to be
183 important for priming the canonical inflammasome pathway, may explain NK cell non
184 responsiveness to NLRP3 triggers and the absence of IL-1β. This differs from the
185 classical activation of these pathways in macrophages where NLRC4 and NLRP3 are
186 major contributors to the innate detection of *Salmonella (43,51,52)*. The inflammatory
187 caspase-dependent secretion of IL-18 is consistent with previous literature showing its
188 cleavage by caspase-4 (9,10,53–55) and suggests that NK cells use an autocrine
189 mechanism to potentiate their activation during bacterial infection.
190
191 ***Salmonella* Typhimurium accesses the cytosol in human NK cells**
192 Gram-negative bacteria can activate the NCI through a range of mechanisms,
193 including direct invasion of the host cell cytoplasm or secretion of outer-membrane
194 vesicles (7). Upon infection of epithelial and myeloid cells, *Salmonella* localises and
195 replicates in specialised vacuoles, where it is protected from immune detection.
196 However, as established in gut epithelial cells, *Salmonella* can escape these vacuoles,
197 allowing cytosolic hyper-replication but also its detection by cytoplasmic sensors (56).
198 Therefore, we next sought to identify whether *Salmonella* invade NK cells by
199 infecting them with *S.* Typhimurium LT2-TdTomato. Using flow cytometry, we showed
200 that ~40% of NK cells were TdTomato$^+$ (**Figure 3A**), suggesting an efficient invasion
201 of NK cells. Moreover, fluorescence microscopy on NK cells indicates the presence of
202 Tdtomato$^+$ *S.* Typhimurium in both CD56$^+$ vacuole-like structures and in the cytosol
203 (**Figure 3B**). We observed a range of NK cell-*Salmonella* interactions as shown in
204 **Supp.Figure 4A**. However, we could not fully differentiate between cytosolic and
205 vacuole-associated *Salmonella*. To confirm that *Salmonella* could access the cytosol,

206 we used *Salmonella* expressing a glucose-6-phosphate-dependent cytosolic eGFP-
207 reporter (9). As glucose-6-phosphate is only accessible in the cytosol, only cytosolic
208 *Salmonella* will express the fluorescent GFP reporter. At 5hrs post-infection, a
209 significant percentage of NK cells (10-15%), were eGFP$^+$ (**Figure 3C**), similar to levels
210 in epithelial cells (9), suggesting that *Salmonella* can invade the cytosol of a proportion
211 of NK cells. This correlates with NCI activation, as shown by western blot for the active
212 caspase-4 p32 cleavage product (13) and the reduction in full-length GSDMD in NK
213 cells in response to *S.* Typhimurium (**Figure 3D**). In comparison, infection with a Gram-
214 positive bacteria, *Staphylococcus* aureus, which is known to activate the canonical
215 inflammasome (57), did not induce caspase-4 cleavage or reduce full-length GSDMD
216 protein.
217 To confirm inflammatory caspase activation, we used the inflammatory caspase
218 activity-based probe FLICA660 and showed that ~5% of total NK cells were FLICA$^+$
219 upon *Salmonella* infection, compared to ~1% in uninfected cells, validating caspase-4
220 activation (**Figure 3E**). In alignment with our previous microscopy and CellView^{TM}
221 analysis indicates a range of activation and infection states, with the existence of
222 FLICA$^+$*Salmonella*-TdTomato$^-$,FLICA$^-$*Salmonella*-TdTomato$^+$,and FLICA$^+$*Salmonella*-
223 TdTomato$^+$ NK cell populations (**Supp. Figure 4C**). To test the potential of NK cells
224 to act as an infectious reservoir for *Salmonella,* we tracked *S.* Typhimurium LT2-
225 TdTomato infection over 14 days. After 5 hrs and 24 hrs, initial infection persists in a
226 significant subset of NK cells, ~25 - 32%. Between day 1 and day 14 post-infection,
227 this proportion decreases from ~30-20% to 10-5% (**Figure 3F**), indicating a small NK
228 population in which *Salmonella* persists. Thus, our study suggests heterogeneity in
229 infective states in NK cells, with persistence, potentially in the vacuole, and access to
230 cytosolic niches. Further study will be required to determine whether these differences
231 in persistence and access are associated with specific NK cell subsets. Overall, these
232 mechanisms converge on *Salmonella's* ability to create an intracellular niche in NK
233 cells.
234
235 **Mouse NK cells do not activate the non-canonical inflammasome**
236 We next asked whether murine NK cells displayed similar features, using published
237 RNA-seq datasets (58), where gene expression changes were measured in innate-
238 like lymphoid populations, as compared to macrophages, following LPS priming. Our
239 analyses showed that, in contrast to humans, mouse NK cells express *Tlr4*. Other

240 non-canonical inflammasome-associated genes, such as *Gbp2*, *Casp4*, and *Gsdmd*,
241 were expressed, similarly to human NK cells and other mouse innate lymphoid
242 populations (**Supp. Figure 5A**) (59). These results were supported by qPCR analysis
243 of murine wild-type splenic NK cells (**Supp. Figure 5B**). In naive NK cells, we detected
244 transcripts for *Casp1*, *Casp4*, *Gbp2*, *Gsdmd*, and *Ninj1*, which was comparable to
245 expression seen in macrophages. Macrophages were additionally found to express
246 transcripts for *Il18*, *Il1b*, and *Il1a* (also upregulated with LPS priming), but these
247 transcripts were absent in NK cells (**Supp. Figure 5C**). In contrast to human NK cells,
248 *Salmonella* infection did not induce cell death in murine NK cells (**Supp. Figure 5D**).
249 Furthermore, we did not detect protein expression of full-length caspase-11 (the
250 murine orthologue of human caspase-4) in NK cells compared with matched
251 neutrophils (**Supp. Figure 5F**). Unlike human NK cells, which express inflammasome
252 components at the gene level, murine NK cells do not express a functional caspase-
253 11 and do not activate the NCI in response to *Salmonella* infection.
254 In contrast, human NK cells do not express TLR4 but instead use the non-
255 canonical inflammasome to detect intracellular bacterial infection. These data highlight
256 a critical difference between human and murine inflammasomes at the cellular level.
257
258 **The non-canonical inflammasome in human NK cells is primed by IL-12**
259 IFNγ priming in non-phagocytic and phagocytic cells has previously been identified to
260 impact NCI activation (9–11). To investigate the effect of IFNγ on NK cells, we primed
261 resting NK cells *in vitro* for 16 hrs with recombinant human IFNγ or with the NK-
262 activating cytokine IL-12. This cytokine is also important for the human response to
263 *Salmonella,* as individuals with a deficiency in IL-12 signalling are especially sensitive
264 to *Salmonella* infection (60–63).
265 Surprisingly, IFNγ did not induce expression of any NCI-related genes (*CASP4*,
266 *CASP1*, *GBP1*, *GBP2*, *GBP5*, *GSDMD*, and *NINJ1*), as compared to unstimulated
267 cells (**Figure 4A - C**). In contrast, IL-12 stimulation resulted in statistically significant
268 increases in *GBP1* and *GSDMD*. Although this did not increase NK cell death, as
269 measured by LDH assay at 5 hrs post-infection (**Figure 4D**), immunoblotting showed
270 increased cleavage of caspase-4 and GSDMD (**Figure 4E**). Ninj1 levels remained
271 unchanged. IL-12 priming significantly increased IFNγ and CCL3 secretion by NK
272 cells, but did not further enhance this response upon *S.* Typhimurium infection (**Figure
273 4F and G**). Importantly, the *Salmonella*-dependent IL-18 secretion previously

observed (**Figure 2E**) was increased upon IL-12, but not IFNγ priming, indicating a potentiation of NCI activity in human NK cells (**Figure 4H**).

Discussion

Inflammasome pathways have been extensively characterised in macrophages and epithelial cells, yet whether lymphocytes engage these signalling platforms remains unclear. Here, we demonstrate that human NK cells possess a functional non-canonical inflammasome (NCI) that enables cell-intrinsic detection of cytosolic Gram-negative bacteria. This finding repositions NK cells from passive recipients of inflammasome-derived cytokines to autonomous and active participants in anti-bacterial immunity. The NK cell NCI displays a species-specific protein profile and is primed by IL-12 rather than IFNγ.

Human NK cells use a limited inflammasome system. They lack the canonical sensors NLRP3 and NLRC4, do not express TLR4, and fail to produce IL-1β upon bacterial infection. Yet they retain functional caspase-4, guanylate-binding proteins (GBP1, GBP2, GBP5), and GSDMD, enabling detection of cytosolic LPS and execution of pyroptosis. The NK NCI produces a specific output profile with IL-18 secretion and inflammatory cell death without IL-1β production, highlighting fundamental differences from macrophage responses to the same pathogen. However, the prevalence of such mechanisms across lymphocyte populations remains to be fully investigated. Previous work suggested that T cell subsets activate the canonical CARD8 inflammasome upon treatment with chemotherapeutics, triggering cell death without cytokine production (38).

Strikingly, murine NK cells, despite expressing inflammasome component transcripts at levels comparable to macrophages, lack functional caspase-11 protein and do not undergo pyroptosis upon *Salmonella* infection. This transcript-protein discordance suggests post-transcriptional or translational regulation that differs between species. This species difference has practical implications: mouse models have been used extensively to study NK cell responses to *Salmonella*, including in cancer immunotherapy contexts (64). Our findings urge caution in extrapolating from these

306 studies to human NK cell biology and suggest that human-specific experimental
307 systems are essential for understanding the contributions of inflammasomes to human
308 NK cell function.

309 The selective responsiveness of human NK cells to IL-12 rather than IFNγ priming
310 represents an unexpected regulatory distinction from other cell types. IFNγ, signalling
311 through JAK-STAT1 (65), is the canonical priming agent for non-canonical
312 inflammasome components in macrophages and epithelial cells (9–11). In NK cells,
313 however, IFNγ had no effect on caspase-4, GBPs, or GSDMD expression. Recent
314 transcriptomic analyses support this interpretation, demonstrating that NK cells show
315 minimal response to IFNγ compared with T and B cells (66). IL-12, via STAT4
316 signalling (61), significantly upregulated these components and enhanced infection-
317 induced IL-18 secretion. This suggests that the promoters of key NCI genes may
318 harbour STAT4-responsive elements that are preferentially active in NK cells. The IL-
319 12 dependency also aligns with clinical observations that individuals with defects in IL-
320 12 signalling are particularly susceptible to *Salmonella* infection, raising the possibility
321 that impaired NK cell inflammasome priming contributes to this phenotype (60,63).

322 Our observation that *Salmonella* infection induces IL-18 secretion from NK cells
323 indicates a potential for autocrine amplification of NK cell responses. IL-18 receptor
324 expression varies across NK cell subsets, with recent single-cell analyses indicating
325 the highest expression in NK2 (CD56high, CD16low) populations. If NCI-competent
326 NK cells (predominantly NK1 and NK3, based on our expression data) secrete IL-18
327 upon infection, this could preferentially activate nearby NK2 cells, thereby amplifying
328 the local immune response across tissues. Such subset-specific interactions deserve
329 investigation, as they may shape NK cell responses to bacterial infection. More
330 broadly, the heterogeneity of inflammasome component expression across NK cell
331 subsets with PYCARD/ASC expression being restricted to NK1B and NK1C,
332 highlighting that different NK populations may have distinct capacities for
333 inflammasome activation, a complexity that functional studies have yet to address.

334 Our finding that a subset of NK cells remains infected with *Salmonella* over 14 days
335 raises questions about bacterial persistence and potential immune evasion.
336 *Salmonella* persistence in macrophage vacuoles is well documented and enables
337 antibiotic evasion and cellular reprogramming (67). Whether similar mechanisms

338 operate in NK cells and whether persistent infection affects NK cell function or
339 memory-like phenotypes remain to be determined. Our data indicate that, at least
340 during the initial infection, *Salmonella* can invade NK cell cytosol and activate the NCI.
341 The absence of NLRP3 and NLRC4 in these cells suggests that cytosolic LPS is likely
342 the primary PAMP sensed by NK cells upon *Salmonella* infection. However, we cannot
343 exclude other inflammatory conditions that may prime caspase-1 activation in these
344 cells (e.g., other pathogens).

345 In conclusion, we have identified a specialised non-canonical inflammasome pathway
346 in human NK cells that operates independently of canonical inflammasome
347 components and is regulated by IL-12 rather than IFNγ. This pathway enables NK cells
348 to directly sense intracellular Gram-negative bacteria, adding to the network of innate
349 immune cells capable of autonomous pathogen detection. The species-specific nature
350 of this response highlights the importance of human experimental systems for
351 understanding NK cell inflammasome biology. Future work should address how this
352 pathway shapes tissue responses to infection and whether it contributes to diseases
353 such as sepsis, in which reduced NK cell numbers are observed and are associated
354 with poor patient outcomes (68).

355

356

357 **Material and Methods**

358 **Study approval**

359 Work with human primary cells was performed under approval by the University of
360 York Biology Ethic Committee (DB202111). Mice were bred and maintained in specific
361 pathogen-free conditions in the University of York, Biological Services Facility. Surplus
362 C57 BL/6 mouse tissue was used with the approval of the local AWERB committee,
363 and under license with the UK Home Office.

364

365 **Human immune cell isolation and expansion**

366 Human NK cells, PBMCs and neutrophils were isolated from fresh blood in EDTA-
367 coated tubes (BD Bioscience) or from blood cones (apheresis product, NHS) collected
368 from anonymous healthy donors. Neutrophils (only from fresh blood) and NK cells
369 were isolated from whole blood by negative selection using the EasySep Direct

370 Neutrophil isolation kit (StemCell Technology, 19666) and EasySep Direct human NK
371 isolation kit (StemCell Technology, 19665). To ensure a maximal NK purity, isolated
372 NK cells were expanded for 14 days with Immunocult NK Cell Expansion Kit (StemCell
373 Technology, 100-0711), according to manufacturer instructions. After 14 days, dead
374 cells from NK culture were removed using EasySep Dead Cell Removal (Annexin V)
375 Kit.
376 PBMCs were isolated from whole blood using Lymphocyte Separation Medium
377 (Lonza, BESP1109E). Red blood cells were lysed using ACK lysis buffer (Gibco,
378 A1049201) for 5 min at room temperature. PBMCs were differentiated into
379 macrophages with 50 ng/ml rhM-CSF (Proteintech, HZ-1192) in RPMI, 10% FBS, 1%
380 penicillin/streptomycin, and 1% glutamine for 7 days at 37°C, 5% CO_2.
381
382 **Murine immune cell isolation and priming**
383 C57BL/6J mouse spleens were collected in PBS with 2% FBS. Single cell suspensions
384 were obtained by passing tissue through a 70µm cell strainer (Corning, 352350). Red
385 blood cells were lysed using ammonium chloride solution for 5 minutes at room
386 temperature. Neutrophils were isolated using an EasySep Direct Neutrophil isolation
387 kit (StemCell Technology, 19855). NK cells
388 (LiveCD45$^+$CD3CD4CD8CD19CD11bCD11cFcεR1Gr1 (lineage)$^-$NK1.1$^+$) and
389 macrophages (LiveCD45$^+$CD3$^-$CD11b^{high}) were stained with flow cytometry antibodies
390 (see **Supplementary Table 1**) and isolated by FACS using a MoFlo Astrios (Beckman
391 Coulter, Summit software). Mouse NK cells and macrophages were primed with 100
392 ng/mL of LPS EK (Invivogen) for 3hrs or used directly for RNA extraction after isolation.
393
394 **Bacterial infection, cell priming, and cell death analysis**
395 NK cells, neutrophils, and differentiated macrophages were plated in 12-well plates in
396 Opti-MEM (GIBCO) at 1x10^6 cells/ml, 2.5x10^6 cells/m and 0.5x10^6 cells/ml,
397 respectively. Cells were infected with either *Salmonella enterica* Serovar Typhimurium
398 SL1344 or LT2, or *S. enterica⊿orgA*, LT2-TdTomato, LT2-pPuhpT-GFP, or
399 *Staphylococcus aureus* grown in log phase. Briefly, bacterial strains were cultured in
400 lysogeny broth (LB) medium overnight at 37°C on an orbital shaker. These were
401 subcultured 1:40 and grown for 3h at 37°C to generate log phase cultures. Before
402 infection, bacteria were collected by centrifugation, and washed twice with pre-warmed
403 PBS. Cells were infected at MOI 50 for 1h at 37°C. After 1 hr, gentamicin was added

404 at a final concentration of 100 µg/ml to kill extracellular bacteria and cells were
405 incubated for 4 hrs at 37°C, 5% CO_2. As indicated, VX-765 (25 µM in DMSO, Sigma-
406 Aldrich, 5.31372) was added 30 mins before inflammasome activation.
407 In some experiments, NK, rested for 6 hours in NK medium without NK cell
408 Expansion Supplement (StemCell Technology, 100-0711) and neutrophils were
409 primed 3 hours with 100 ng/ml ultrapure LPS-EK (Invivogen, tlrl-peklps) or with 25
410 ng/ml rhIFNγ (Proteintech, HZ-1301) or 100 ng/ml rhIL-12 (Proteintech, HZ-1256) for
411 16 hours. NLRP3 inflammasome was activated using Nigericin (20 µM in EtOH,
412 Sigma-Aldrich, N7143) for 3 hrs at 37°C. As indicated MCC950 (10 µM in H_2O, Sigma-
413 Aldrich, PZ0280) were added to the cell culture media 30 min before inflammasome
414 activation. NLRP1 was activated using 3 µM Val-boroPro for 6 hrs at 37°C (Vbp,
415 5.31465).
416 For cell death measurements lactate dehydrogenase release in the
417 supernatants was measured using a CytoTox 96® Non-Radioactive Cytotoxicity
418 Assay (Promega, G1780). Absorbance was measured on a plate reader (Infinite M
419 Plex, TECAN) at 490nm with a 650nm background subtraction following
420 manufacturer's instructions.
421
422 **Quantitative PCR analysis**
423 mRNA from primary cells (mouse and human) were isolated using the Arcturus
424 PicoPure Isolation kit (ThermoFisher, KIT0204) and cDNA was generated using the
425 SuperScript IV First Strand kit (ThermoFischer, 18091050), using manufacturer's
426 instructions. qPCR was performed using TaqMan probes (Life Technologies,
427 **Supplementary Table 1**) on an AriaMx Real-time PCR system (Agilent).
428
429 **Immunoblotting**
430 Cell extracts were lysed with cell sample buffer (2% SDS, 66mM Tris pH7.6
431 reconstituted in NuPage 1X LDS buffer (Novex, P5878547) and run on 10% or 4 - 20%
432 acrylamide gels (BioRad) with methanol-chloroform precipitated cell supernatant
433 mixes (69). Gels were transferred on 45 µM nitrocellulose membrane using the
434 TurboBlot transfer system (BioRad), and blocked in 5% skimmed milk TBST. Samples
435 were then incubated overnight at room temperature in the primary antibody at 4°C and
436 for 2 hrs the following day in the secondary antibody (**Supplementary Table 1**).

437 Membrane was imaged using the Immobilon Forte ECL Substrate (VWR, WBLUF)
438 using a ThermoFisher iBright 1500.
439
440 **Flow cytometry**
441 Single cell suspensions were incubated with anti-CD16/CD32 antibodies (Biolegend,
442 Clone 93) followed by fluorochrome-conjugated antibodies as detailed in
443 **Supplementary Table 1**. All samples were co-stained with a cell viability dye (Zombie
444 YG581 or Aqua, Biolegend, 423123 and 423102). In some experiments with human
445 blood NK cells after *Salmonella* infection, and following the addition of gentamicin,
446 YVAD-FMK FLICA660 or FLICA-FAM was added following manufacturer instructions
447 (1:1000, FLICA Caspase-1 kit, BIO-RAD, 9120 and ICT098) and cells were incubated
448 for 1 hr at 37°C. Cells were washed twice with the 1x kit wash buffer. Untreated NK
449 cells stained for FLICA were used as control. Sample acquisition used an LSR
450 Fortessa, CytoFLEX LX (Beckman Coulter), or FACSDiscover™ S8 (BD Biosciences,
451 CellView™ Image) and then visualised using FlowJo (version 10.10) software. For
452 cell sorting, an Astrios (70 µm nozzle, Beckman Coulter, Summit software) was used.
453
454 **Immunofluorescence microscopy**
455 8-well chamber slides (Ibidi, 80821) were coated with 12.5 µg/ml fibronectin for 1 hr,
456 washed with PBS and transferred to 4°C until use. NK cells were seeded directly into
457 chamber slides at $4x10^5$ cells/well and immediately infected with log phase *Salmonella*
458 LT2-TdTomato at MOI 50 for 1h at 37°C, 5% CO_2. Gentamicin was added directly to
459 the culture medium, and cells were cultured for 4 hrs at 37°C, 5% CO_2. Cells were
460 subsequently fixed with 4% PFA (in PBS) for 10 min at room temperature and washed
461 with PBS. Cells were blocked with 5% goat serum for 2 hrs, stained with rabbit anti-
462 human NCAM (CD56, Cell Signalling, 99746) overnight, washed with PBS and stained
463 with goat anti-rabbit IgG (H+L), AF488 conjugate (Cell Signalling, 4412) for 1 hr. Cells
464 were washed with PBS and stained with DAPI (2µg/ml) (Biotum, 40043), ready for
465 imaging on Zeiss Elyra 7.
466
467 **Cytokine assays**
468 Cytokine secretion in cell culture supernatants was assessed using standard sandwich
469 ELISA, IL-1β (Invitrogen, 88-7261), CCL3 (Invitrogen, 88-7035) , IL-18 (R&D systems,
470 DY318-05), GM-CSF (Invitrogen, 88-8337), IL-22 (Invitrogen, 88-7522), according to

471 the manufacturer's instructions. IFNγ secretion was measured using the Lumit IFNγ
472 immunoassay (Promega, W6040) following the manufacturer's instructions in a 384
473 well plate. Luminescence was measured on a plate reader (Infinite M Plex, TECAN).
474
475 **Bioinformatical data analysis and statistics**
476 Mouse RNA sequencing data was obtained from the GEO database (GSE143943,
477 (49). The data was filtered for genes relevant to NCI and the mean expression values
478 log transformed. Heat maps were generated in R Studio using the pheatmap package.
479 Clustering was automatically applied to the gene list.
480 Human scRNAseq datasets were obtained from either the foetal immune cell
481 atlas (https://developmental.cellatlas.io/#) or peripheral blood (https://storage.
482 googleapis.com/haniffalab/meta-nk/PBMC_Noreg.h5ad) and mined to analyse tissue
483 resident or blood NK cells, respectively. The published data was loaded with *scanpy*
484 and the inflammasome component genes visualised in a violin or *dotplot*. The dotplot
485 was grouped by the 6 NK clusters discovered in the original study, and the genes were
486 standard-scaled across these clusters to visualize relative abundance of each gene
487 across cell contexts.
488 Statistical analysis for most experiments was performed using Prism10
489 (GraphPad, San Diego, CA).
490
491
492 **Acknowledgement**
493 D.B. is supported by an MRC New Investigator Award (MR/Z504221/1), a Springboard
494 Award (Academy of Medical Sciences and Wellcome Trust) and a Royal Society
495 Grant. J.A. was supported by a GenerationResearch MSc Studentship and VISFO.
496 J.L.B., D.G.K, and M.C. are supported by the NIHR Leeds Biomedical Research
497 Centre (BRC) (NIHR203331), and J.L.B and D.G.K. by an MRC National Mouse
498 Genetics Network grant (MC_PC_21043). D.G.K is additionally supported by a CRUK
499 Programme Foundation Award (DCRPGF\100008), an MRC-AMED joint award
500 (MR/V005502/1), and Blood Cancer UK (24014). M.G. was in receipt of a BBSRC
501 White Rose DTP PhD Studentship (BB/T007222/1).
502 W.G. is supported by an MRC Career Development Fellowship (MR/X007146/1),
503 Leukaemia U.K. (2021/JGF/002), an EHA bilateral collaborative award and the
504 Children's Cancer and Leukaemia Group (CCLGA 2022 13 Grey). K.S.R is supported

by the Academy of Medical Sciences Springboard (SBF009\1153), Royal Society (RG\R1\241058) and Hull York Medical School Start-up. The authors thank the Centre for Blood Research (CBR), SUKIT and the InflammaZoom UK networks for helpful discussions and constructive criticism on this research. The authors thank the phlebotomist team at the University of York for their support with collecting fresh blood for experimental purposes and the donors who kindly provided the blood. N/TERT was a kind donation from Prof. James Rheinwald (70). We would like to thank Prof. Petr Broz (University of Lausanne) and Prof. Marjan van der Woude (University of York) for providing the bacterial strains used in this study.

Authors contribution

N.G.F.L, J.A, A.H, Z.A, K.S.R, M.G, C.R, A.V, J.L.B, M.A.C, F.P. and D.B performed experiments. N.G.F.L, Z.A, J.H, J.L.B and D.B designed experiments, D.B secured funding, supervised, designed and oversaw the project. N.G.F.L, J.A, A.H, K.S.R, K.H, G.C, J.L.B, D.B analysed data. D.B, N.G.F.L, and J.L.B wrote the paper with inputs from all authors.

521 **References**

522 1. Janeway CA. Approaching the asymptote? Evolution and revolution in immunology. Cold
523 Spring Harb Symp Quant Biol. 1989;54 Pt 1:1–13.

524 2. Fu J, Schroder K, Wu H. Mechanistic insights from inflammasome structures. Nat Rev
525 Immunol. 2024 July;24(7):518–35.

526 3. Schroder K, Tschopp J. The inflammasomes. Cell. 2010 Mar 19;140(6):821–32.

527 4. Ross C, Chan AH, von Pein JB, Maddugoda MP, Boucher D, Schroder K. Inflammatory
528 Caspases: Toward a Unified Model for Caspase Activation by Inflammasomes. Annu Rev
529 Immunol. 2022 Apr 26;40:249–69.

530 5. Rathinam VAK, Zhao Y, Shao F. Innate immunity to intracellular LPS. Nat Immunol. 2019
531 May;20(5):527–33.

532 6. Grant S, Boucher D. 10 things you wish you knew about inflammatory caspases: a holistic
533 review of their biochemistry, activation, and signalling. J Biol Chem. 2025 Aug 2;110557.

534 7. Vanaja SK, Russo AJ, Behl B, Banerjee I, Yankova M, Deshmukh SD, et al. Bacterial
535 Outer Membrane Vesicles Mediate Cytosolic Localization of LPS and Caspase-11
536 Activation. Cell. 2016 May;165(5):1106–19.

537 8. Tretina K, Park ES, Maminska A, MacMicking JD. Interferon-induced guanylate-binding
538 proteins: Guardians of host defense in health and disease. J Exp Med. 2019 Mar
539 4;216(3):482–500.

540 9. Santos JC, Boucher D, Schneider LK, Demarco B, Dilucca M, Shkarina K, et al. Human
541 GBP1 binds LPS to initiate assembly of a caspase-4 activating platform on cytosolic
542 bacteria. Nat Commun. 2020 June 24;11(1):3276.

543 10. Wandel MP, Kim BH, Park ES, Boyle KB, Nayak K, Lagrange B, et al. Guanylate-
544 binding proteins convert cytosolic bacteria into caspase-4 signaling platforms. Nat
545 Immunol. 2020 Aug;21(8):880–91.

546 11. Fisch D, Bando H, Clough B, Hornung V, Yamamoto M, Shenoy AR, et al. Human
547 GBP1 is a microbe-specific gatekeeper of macrophage apoptosis and pyroptosis. EMBO
548 J. 2019 July 1;38(13):e100926.

549 12. Kutsch M, Sistemich L, Lesser CF, Goldberg MB, Herrmann C, Coers J. Direct
550 binding of polymeric GBP1 to LPS disrupts bacterial cell envelope functions. EMBO J.
551 2020 July 1;39(13):e104926.

552 13. Chan AH, Burgener SS, Vezyrgiannis K, Wang X, Acklam J, Von Pein JB, et al.
553 Caspase-4 dimerisation and D289 auto-processing elicit an interleukin-1β-converting
554 enzyme. Life Sci Alliance. 2023 Oct;6(10):e202301908.

555 14. Broz P, Pelegrín P, Shao F. The gasdermins, a protein family executing cell death
556 and inflammation. Nat Rev Immunol. 2020 Mar;20(3):143–57.

557 15. Shi J, Zhao Y, Wang K, Shi X, Wang Y, Huang H, et al. Cleavage of GSDMD by
558 inflammatory caspases determines pyroptotic cell death. Nature. 2015 Oct
559 29;526(7575):660–5.

560 16. Kayagaki N, Stowe IB, Lee BL, O'Rourke K, Anderson K, Warming S, et al. Caspase-
561 11 cleaves gasdermin D for non-canonical inflammasome signalling. Nature. 2015 Oct
562 29;526(7575):666–71.

563 17. Kayagaki N, Kornfeld OS, Lee BL, Stowe IB, O'Rourke K, Li Q, et al. NINJ1 mediates
564 plasma membrane rupture during lytic cell death. Nature. 2021 Mar;591(7848):131–6.

565 18. Chen KW, Broz P. Gasdermins as evolutionarily conserved executors of
566 inflammation and cell death. Nat Cell Biol. 2024 Sept;26(9):1394–406.

567 19. Deets KA, Vance RE. Inflammasomes and adaptive immune responses. Nat
568 Immunol. 2021 Apr;22(4):412–22.

569 20. Rühl S, Broz P. Caspase-11 activates a canonical NLRP3 inflammasome by
570 promoting K(+) efflux. Eur J Immunol. 2015 Oct;45(10):2927–36.

571 21. Baker PJ, Boucher D, Bierschenk D, Tebartz C, Whitney PG, D'Silva DB, et al.
572 NLRP3 inflammasome activation downstream of cytoplasmic LPS recognition by both
573 caspase-4 and caspase-5. Eur J Immunol. 2015 Oct;45(10):2918–26.

574 22. Schmid-Burgk JL, Gaidt MM, Schmidt T, Ebert TS, Bartok E, Hornung V. Caspase-4
575 mediates non-canonical activation of the NLRP3 inflammasome in human myeloid cells.
576 Eur J Immunol. 2015 Oct;45(10):2911–7.

577 23. Monteleone M, Stanley AC, Chen KW, Brown DL, Bezbradica JS, von Pein JB, et al.
578 Interleukin-1β Maturation Triggers Its Relocation to the Plasma Membrane for Gasdermin-
579 D-Dependent and -Independent Secretion. Cell Rep. 2018 Aug 7;24(6):1425–33.

580 24. Evavold CL, Ruan J, Tan Y, Xia S, Wu H, Kagan JC. The Pore-Forming Protein
581 Gasdermin D Regulates Interleukin-1 Secretion from Living Macrophages. Immunity.
582 2018 Jan 16;48(1):35-44.e6.

583 25. Chan AH, Schroder K. Inflammasome signaling and regulation of interleukin-1 family
584 cytokines. J Exp Med. 2020 Jan 6;217(1):e20190314.

585 26. Vivier E, Artis D, Colonna M, Diefenbach A, Di Santo JP, Eberl G, et al. Innate
586 Lymphoid Cells: 10 Years On. Cell. 2018 Aug 23;174(5):1054–66.

587 27. Tang F, Li J, Qi L, Liu D, Bo Y, Qin S, et al. A pan-cancer single-cell panorama of
588 human natural killer cells. Cell. 2023 Sept;186(19):4235-4251.e20.

589 28. Lanier LL, Le AM, Civin CI, Loken MR, Phillips JH. The relationship of CD16 (Leu-11)
590 and Leu-19 (NKH-1) antigen expression on human peripheral blood NK cells and
591 cytotoxic T lymphocytes. J Immunol Baltim Md 1950. 1986 June 15;136(12):4480–6.

592 29. Nagler A, Lanier LL, Cwirla S, Phillips JH. Comparative studies of human FcRIII-
593 positive and negative natural killer cells. J Immunol Baltim Md 1950. 1989 Nov
594 15;143(10):3183–91.

595 30. Lusty E, Poznanski SM, Kwofie K, Mandur TS, Lee DA, Richards CD, et al. IL-18/IL-
596 15/IL-12 synergy induces elevated and prolonged IFN-γ production by ex vivo expanded
597 NK cells which is not due to enhanced STAT4 activation. Mol Immunol. 2017 Aug;88:138–
598 47.

31. Hook CE, Matyszak MK, Gaston JSH. Infection of epithelial and dendritic cells by *Chlamydia trachomatis* results in IL-18 and IL-12 production, leading to interferon-Î³ production by human natural killer cells. FEMS Immunol Med Microbiol. 2005 Aug;45(2):113–20.

32. Humann J, Lenz LL. Activation of Naive NK Cells in Response to *Listeria monocytogenes* Requires IL-18 and Contact with Infected Dendritic Cells. J Immunol. 2010 May 1;184(9):5172–8.

33. Esin S, Batoni G, Counoupas C, Stringaro A, Brancatisano FL, Colone M, et al. Direct Binding of Human NK Cell Natural Cytotoxicity Receptor NKp44 to the Surfaces of Mycobacteria and Other Bacteria. Infect Immun. 2008 Apr;76(4):1719–27.

34. Chalifour A, Jeannin P, Gauchat JF, Blaecke A, Malissard M, N'Guyen T, et al. Direct bacterial protein PAMP recognition by human NK cells involves TLRs and triggers α-defensin production. Blood. 2004 Sept 15;104(6):1778–83.

35. Reinke S, Pantazi E, Chappell GR, Sanchez-Martinez A, Guyon R, Fergusson JR, et al. Emulsion and liposome-based adjuvanted R21 vaccine formulations mediate protection against malaria through distinct immune mechanisms. Cell Rep Med. 2023 Nov 21;4(11):101245.

36. Muñoz-Wolf N, Ward RW, Hearnden CH, Sharp FA, Geoghegan J, O'Grady K, et al. Non-canonical inflammasome activation mediates the adjuvanticity of nanoparticles. Cell Rep Med. 2023 Jan;4(1):100899.

37. Linder A, Hornung V. Inflammasomes in T cells. J Mol Biol. 2022 Feb 28;434(4):167275.

38. Linder A, Bauernfried S, Cheng Y, Albanese M, Jung C, Keppler OT, et al. CARD8 inflammasome activation triggers pyroptosis in human T cells. EMBO J. 2020 Oct 1;39(19):e105071.

39. Kroes MM, Mariman R, Hijdra D, Hamstra HJ, Van Boxtel KJWM, Van Putten JPM, et al. Activation of Human NK Cells by Bordetella pertussis Requires Inflammasome Activation in Macrophages. Front Immunol. 2019 Aug 27;10:2030.

40. Bierschenk D, Boucher D, Schroder K. Salmonella-induced inflammasome activation in humans. Mol Immunol. 2017 June;86:38–43.

41. Clare B. Inflammasome activation by Salmonella. Curr Opin Microbiol. 2021 Dec;64:27–32.

42. Rebuffet L, Melsen JE, Escalière B, Basurto-Lozada D, Bhandoola A, Björkström NK, et al. High-dimensional single-cell analysis of human natural killer cell heterogeneity. Nat Immunol. 2024 Aug;25(8):1474–88.

43. Gram AM, Wright JA, Pickering RJ, Lam NL, Booty LM, Webster SJ, et al. Salmonella Flagellin Activates NAIP/NLRC4 and Canonical NLRP3 Inflammasomes in Human Macrophages. J Immunol Baltim Md 1950. 2021 Feb 1;206(3):631–40.

44. Naseer N, Egan MS, Reyes Ruiz VM, Scott WP, Hunter EN, Demissie T, et al. Human NAIP/NLRC4 and NLRP3 inflammasomes detect Salmonella type III secretion system activities to restrict intracellular bacterial replication. PLoS Pathog. 2022 Jan;18(1):e1009718.

641 45. Naschberger E, Geißdörfer W, Bogdan C, Tripal P, Kremmer E, Stürzl M, et al.
642 Processing and secretion of guanylate binding protein-1 depend on inflammatory caspase
643 activity. J Cell Mol Med. 2017 Sept;21(9):1954–66.

644 46. Wannamaker W, Davies R, Namchuk M, Pollard J, Ford P, Ku G, et al. (S)-1-((S)-2-
645 {[1-(4-Amino-3-chloro-phenyl)-methanoyl]-amino}-3,3-dimethyl-butanoyl)-pyrrolidine-2-
646 carboxylic acid ((2 R,3 S)-2-ethoxy-5-oxo-tetrahydro-furan-3-yl)-amide (VX-765), an Orally
647 Available Selective Interleukin (IL)-Converting Enzyme/Caspase-1 Inhibitor, Exhibits
648 Potent Anti-Inflammatory Activities by Inhibiting the Release of IL-1β and IL-18. J
649 Pharmacol Exp Ther. 2007 May;321(2):509–16.

650 47. Srikanth CV, Mercado-Lubo R, Hallstrom K, McCormick BA. Salmonella effector
651 proteins and host-cell responses. Cell Mol Life Sci CMLS. 2011 Nov;68(22):3687–97.

652 48. Agbor TA, McCormick BA. Salmonella effectors: important players modulating host
653 cell function during infection. Cell Microbiol. 2011 Dec;13(12):1858–69.

654 49. Coll RC, Hill JR, Day CJ, Zamoshnikova A, Boucher D, Massey NL, et al. MCC950
655 directly targets the NLRP3 ATP-hydrolysis motif for inflammasome inhibition. Nat Chem
656 Biol. 2019 June;15(6):556–9.

657 50. Okondo MC, Johnson DC, Sridharan R, Go EB, Chui AJ, Wang MS, et al. DPP8 and
658 DPP9 inhibition induces pro-caspase-1-dependent monocyte and macrophage pyroptosis.
659 Nat Chem Biol. 2017 Jan;13(1):46–53.

660 51. Man SM, Hopkins LJ, Nugent E, Cox S, Glück IM, Tourlomousis P, et al.
661 Inflammasome activation causes dual recruitment of NLRC4 and NLRP3 to the same
662 macromolecular complex. Proc Natl Acad Sci U S A. 2014 May 20;111(20):7403–8.

663 52. Miao EA, Alpuche-Aranda CM, Dors M, Clark AE, Bader MW, Miller SI, et al.
664 Cytoplasmic flagellin activates caspase-1 and secretion of interleukin 1beta via Ipaf. Nat
665 Immunol. 2006 June;7(6):569–75.

666 53. Wang K, Sun Q, Zhong X, Zeng M, Zeng H, Shi X, et al. Structural Mechanism for
667 GSDMD Targeting by Autoprocessed Caspases in Pyroptosis. Cell. 2020 Mar
668 5;180(5):941-955.e20.

669 54. Devant P, Dong Y, Mintseris J, Ma W, Gygi SP, Wu H, et al. Structural insights into
670 cytokine cleavage by inflammatory caspase-4. Nature. 2023 Dec;624(7991):451–9.

671 55. Exconde PM, Hernandez-Chavez C, Bourne CM, Richards RM, Bray MB, Lopez JL,
672 et al. The tetrapeptide sequence of IL-18 and IL-1β regulates their recruitment and
673 activation by inflammatory caspases. Cell Rep. 2023 Dec 26;42(12):113581.

674 56. Chong A, Cooper KG, Kari L, Nilsson OR, Hillman C, Fleming BA, et al. Cytosolic
675 replication in epithelial cells fuels intestinal expansion and chronic fecal shedding of
676 Salmonella Typhimurium. Cell Host Microbe. 2021 July;29(7):1177-1185.e6.

677 57. Craven RR, Gao X, Allen IC, Gris D, Wardenburg JB, McElvania-TeKippe E, et al.
678 Staphylococcus aureus α-Hemolysin Activates the NLRP3-Inflammasome in Human and
679 Mouse Monocytic Cells. Ratner AJ, editor. PLoS ONE. 2009 Oct 14;4(10):e7446.

680 58. Kim EY, Ner-Gaon H, Varon J, Cullen AM, Guo J, Choi J, et al. Post-sepsis
681 immunosuppression depends on NKT cell regulation of mTOR/IFN-γ in NK cells. J Clin
682 Invest. 2020 June 1;130(6):3238–52.

683 59. Yang S, Sheffer M, Kaplan IE, Wang Z, Tarannum M, Dinh K, et al. Non-pathogenic
684 E. coli displaying decoy-resistant IL18 mutein boosts anti-tumor and CAR NK cell
685 responses. Nat Biotechnol. 2024 Oct 4;

686 60. Jong RD, Altare F, Haagen IA, Elferink DG, Boer TD, Van Breda Vriesman PJC, et
687 al. Severe Mycobacterial and *Salmonella* Infections in Interleukin-12 Receptor-Deficient
688 Patients. Science. 1998 May 29;280(5368):1435–8.

689 61. Tait Wojno ED, Hunter CA, Stumhofer JS. The Immunobiology of the Interleukin-12
690 Family: Room for Discovery. Immunity. 2019 Apr;50(4):851–70.

691 62. Ottenhoff THM, Verreck FAW, Lichtenauer-Kaligis EGR, Hoeve MA, Sanal O, van
692 Dissel JT. Genetics, cytokines and human infectious disease: lessons from weakly
693 pathogenic mycobacteria and salmonellae. Nat Genet. 2002 Sept;32(1):97–105.

694 63. Staretz-Haham O, Melamed R, Lifshitz M, Porat N, Fieschi C, Casanova JL, et al.
695 Interleukin-12 Receptor β1 Deficiency Presenting as Recurrent Salmonella Infection. Clin
696 Infect Dis. 2003 July 1;37(1):137–40.

697 64. Lin Q, Rong L, Jia X, Li R, Yu B, Hu J, et al. IFN-γ-dependent NK cell activation is
698 essential to metastasis suppression by engineered Salmonella. Nat Commun. 2021 May
699 5;12(1):2537.

700 65. Schroder K, Hertzog PJ, Ravasi T, Hume DA. Interferon-gamma: an overview of
701 signals, mechanisms and functions. J Leukoc Biol. 2004 Feb;75(2):163–89.

702 66. Moss N, Sakai C, Kaul SN, Graybuck LT, Rachid Zaim S, Angus-Hill ML, et al.
703 Dissecting type I and II interferon impacts on human immune cells in disease by a cell
704 type-specific interferon response atlas [Internet]. Immunology; 2025 [cited 2026 Jan 20].
705 Available from: http://biorxiv.org/lookup/doi/10.64898/2025.12.02.691676

706 67. Stapels DAC, Hill PWS, Westermann AJ, Fisher RA, Thurston TL, Saliba AE, et al.
707 *Salmonella* persisters undermine host immune defenses during antibiotic treatment.
708 Science. 2018 Dec 7;362(6419):1156–60.

709 68. Andaluz-Ojeda D, Iglesias V, Bobillo F, Almansa R, Rico L, Gandía F, et al. Early
710 natural killer cell counts in blood predict mortality in severe sepsis. Crit Care. 2011 Oct
711 21;15(5):R243.

712 69. Groß O. Measuring the Inflammasome. In: Ashman RB, editor. Leucocytes [Internet].
713 Totowa, NJ: Humana Press; 2012 [cited 2025 July 6]. p. 199–222. (Methods in Molecular
714 Biology; vol. 844). Available from: https://link.springer.com/10.1007/978-1-61779-527-
715 5_15

716 70. Dickson MA, Hahn WC, Ino Y, Ronfard V, Wu JY, Weinberg RA, et al. Human
717 Keratinocytes That Express hTERT and Also Bypass a $p16^{INK4a}$ -Enforced Mechanism
718 That Limits Life Span Become Immortal yet Retain Normal Growth and Differentiation
719 Characteristics. Mol Cell Biol. 2000 Feb 1;20(4):1436–47.

720

721

722 **Figure 1. Human blood NK cells express components of the non-canonical**
723 **inflammasome.** (**A**) scRNA-seq data of inflammasome components in subsets of
724 human peripheral blood NK cells showing the relative abundance (standard-scaled)
725 and percentage of cells expressing inflammasome components, (n=19). (**B**)
726 Quantitative PCR analysis of non-canonical inflammasome components in
727 unexpanded human peripheral blood NK cells, n = 4 donors (**C**) Quantitative PCR
728 analysis of *TLR4* and *NLRP3* in unexpanded peripheral blood NK cells and neutrophils
729 from four matched donors. (**D**) Western blot analysis of expanded human peripheral
730 blood NK cells and macrophages from 2 matched donors compared to loading controls
731 of αTubulin and H3. *[1] and *[2] indicate NK cell-specific protein isoforms of GBP1 and
732 GBP5, respectively. Western blot is representative of 4 blood donors.
733
734 **Figure 2. *Salmonella* Typhimurium infection induces cell death and IL-18**
735 **production in human blood NK cells.** Expanded human peripheral blood NK cells
736 were infected with *S.* Typhimurium or *S.* Typhimurium*⊿orgA*, and with or without VX-
737 765. At 5 hrs post-infection, cells supernatants were assessed by (**A** and **B**) LDH assay
738 for cell death, and (**D** and **E**) ELISA for IL-1beta and IL-18 production, n = 6 - 9 donors
739 across 2 - 3 independent experiments. (**C**) Quantitative PCR analysis of *IL1B* following
740 priming with LPS (for 3 hrs) and IFNgamma (for 16 hrs). **(F)** At 5 hrs post-infection,
741 caspase-1 cleavage was characterised by western blot. *[1] indicate a p33 cleavage
742 product of active caspase-1. In (**C**), (**D**) and (**F**) NK cells were compared to neutrophils
743 and macrophages from matching donors. Data in (A, B and E) were analysed by one-
744 way ANOVA with Dunnett's multiple-comparison test. p values are displayed and
745 $p<0.05$ was considered statistically significant.
746
747 **Figure 3. *Salmonella* Typhimurium accesses the cytosol and persists in human**
748 **blood NK cells.** Expanded human peripheral blood NK cells were infected with *S.*
749 Typhimurium-TdTomato. (**A**) At 5 hrs post-infection NK cells were subjected to
750 analysis by flow cytometry or (**B**), stained on fibronectin coated slides with anti-CD56
751 and DAPI and visualised by fluorescence microscopy (white bar indicates 5 µm). (**C**)
752 Alternatively, these NK cells were infected with *S.* Typhimurium, stably expressing a
753 cytosolic-induced eGFP reporter and analysed by flow cytometry. (**D**) Representative
754 western blot analysis of expanded human peripheral blood NK cells infected with either
755 *S.* Typhimurium or *Staphylococcus* aureus and with or without VX-765 for 5 hrs

compared to loading controls of H3. *[1] indicates a p32 cleavage product of active caspase-4 (**E**) Caspase-1 and -4 activation was measured by flow cytometry using the inflammatory caspase probe FLICA660 . (**F**) Percentage of *S.* Typhimurium-TdTomato in NK cells was measured at days 1, 2, 5, 7, and 14 post-infection. Data from 2 independent experiments, n = 4 - 6 donors. Data in (A, C and E) were analysed by paired t tests. Data in (F) were analysed by one-way ANOVA with Dunnett's multiple-comparison test. p values are displayed and $p<0.05$ was considered statistically significant.

Figure 4. IL-12 but not IFNγ-mediated activation of human blood NK cells leads to upregulation of non-canonical inflammasome components. Expanded human peripheral blood NK cells were treated with and without rhIL-12 or rhIFNγ for 16 hrs. Quantitative PCR was used to assess expression of (**A**) *CASP4* and *CASP1*, (**B**) *GBP1* and *GBP2*, and (**C**) *GBP5*, *GSDMD*, and *NINJ1*. Post-treatment, NK cells were additionally infected with *S.* Typhimurium alone, or in combination with VX-765. Supernatant was taken at 5 hrs post-infection in order to assess (**D**) cell death by LDH release and (**F**) IFNγ, (**G**) CCL3, and (**H**) IL-18 production by ELISA. (**E**) Representative western blot analysis of expanded and primed human NK cells infected with either *S.* Typhimurium alone or in combination with VX-765 for 5 hrs compared to loading controls of H3. *[1] indicates a p32 cleavage product of caspase-4. *[2] indicates a p30 cleavage product of GSDMD. Data from 2 - 3 independent experiments, n = 3 - 8 donors. Data in (A, B C and H) were analysed by one-way ANOVA with Dunnett's multiple-comparison test. p values are displayed and $p<0.05$ was considered statistically significant.

783 **Supplementary Figure Legends**

784

785 **Supplementary Table 1.** (**A**) Quantitative PCR Taqman primer sets for human and
786 mouse targets. (**B**) Antibodies used in flow cytometry (FC), immunofluorescence (IF),
787 and western blot (WB).

788

789 **Supplementary Figure 1. Human thymic NK cells express components of the**
790 **non-canonical inflammasome.** (**A**) scRNA-seq data of inflammasome components
791 in *CASP4*$^{+}$*GBP2*$^{+}$ and *CASP4*$^{-}$*GBP2*$^{-}$ human foetal thymic non-cycling and cycling NK
792 cells showing the median expression and number of cells expressing inflammasome
793 components. (**B**) Quantitative PCR analysis of non-canonical inflammasome
794 components in neutrophils, n = 4 donors, matched with NK cell phenotypes in Fig. 1B.

795

796 **Supplementary Figure 2. Characterisation of NK cell subpopulations in human**
797 **blood.** Representative density plots of (**A**) PBMCs , (**B**) negatively-selected NK cells
798 and (**C**) 14 days expanded NK cells from human peripheral blood showing typical
799 percentages of CD56^{int}CD16^{+} and CD56^{high}CD16^{-} .
800 Human peripheral blood from (**C**) before and (**D**) after NK cell negative selection,
801 analysed by flow cytometry to show typical percentages of CD56^{int}CD16^{+} and
802 CD56^{high}CD16^{-}, and within this NK1, NK2, and NK3 subsets, as defined by Rebuffet
803 *et al* (2024).

804

805 **Supplementary Figure 3. NLRP1, NLRP3, and FLICA activation in human blood**
806 **NK cells.** Expanded human peripheral blood NK cells were treated with nigericin (20
807 μM), with or without MCC950 (10 μM) for 3 hrs. Cells were then assessed for (**A**) the
808 release of LDH for cell death and (**B**) the cleavage of caspase-1 by western blot. (**C**)
809 NK cells or (**D**) N/TERT keratinocytes were treated with Val-boroPro (3μM, VbP) for
810 6hrs, with and without VX-765, and assessed by western blot. n = 4 - 6 donors. *[1] and
811 *[2] indicate possible NK cell-specific protein isoforms of CASPASE-1. *[3] indicates the
812 p30 cleavage fragment of GSDMD. Data in (A) were analysed by one-way ANOVA
813 with Dunnett's multiple-comparison test. p values are displayed and $p<0.05$ was
814 considered statistically significant.

815

816

817 **Supplementary Figure 4. *Salmonella* Typhimurium interacts with and enters NK**
818 **cells, activating inflammatory caspases.** Expanded human peripheral blood NK
819 cells were infected with *S.* Typhimurium-TdTomato. (**A**) At 5 hrs post-infection NK cells
820 were stained on fibronectin coated slides with anti-CD56 and DAPI and visualised by
821 fluorescence microscopy (white bar indicates 5 μm). Panel shows range of NK cell-
822 *Salmonella* interactions. Control represents non-infected NK cells stained with anti-
823 CD56 and DAPI. (**B**) Representative images of $CD56^+$ cells were reconstructed, using
824 CellView^{TM} beam-splitting technology, to show human NK cells that were FLICA-
825 FAM^+*Salmonella*- $TdTomato^-$ (NK cell 1), FLICA-FAM^-*Salmonella*-$TdTomato^+$ (NK cell
826 2), and FLICA-FAM^+*Salmonella*-$TdTomato^+$ (NK cell 3), respectively.
827
828 **Supplementary Figure 5. Canonical and non-canonical inflammasome**
829 **components are expressed in mouse NK cells at the gene, but not the protein**
830 **level** . (**A**) RNASeq dataset extracted from flow cytometry sorted immune cells
831 showing a heatmap expression analysis of canonical and non-canonical
832 inflammasome-associated genes (58). Murine spleen NK cells and $CD11b^{high}$ cells
833 were sorted and cDNA was extracted from either (**B**) naive populations or (**C**) from
834 LPS (100 ng/mL, 3 hrs)-primed cells. Expression of canonical and non-canonical
835 inflammasome-associated genes was assessed by quantitative PCR using *Gapdh* as
836 a house-keeping gene, n = 4-8, collected across 2 independent experiments. (**D**)
837 Representative western blot analysis of caspase-11 expression in LPS-primed murine
838 spleen NK cells.
839
840

Figure 1

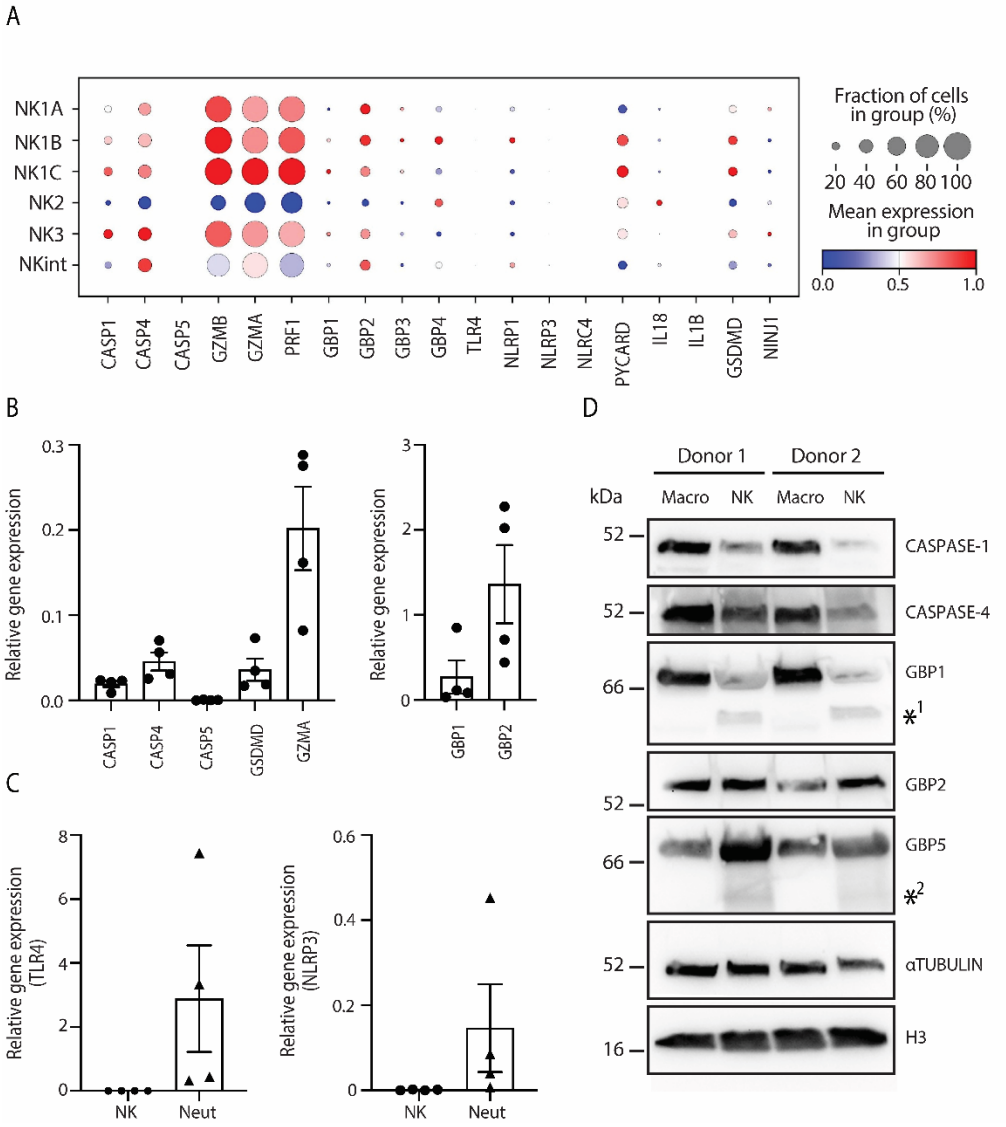
A
NK1A
NK1B
NK1C
NK2
NK3
NKint
CASP1
CASP4
CASP5
GZMB
GZMA
PRF1
GBP1
GBP2
GBP3
GBP4
TLR4
NLRP1
NLRP3
NLRC4
PYCARD
IL18
IL1B
GSDMD
NINJ1
Fraction of cells in group (%)
20 40 60 80 100
Mean expression in group
0.0 0.5 1.0
B
Relative gene expression
CASP1
CASP4
CASP5
GSDMD
GZMA
GBP1
GBP2
C
Relative gene expression (TLR4)
Relative gene expression (NLRP3)
NK
Neut
D
Donor 1
Donor 2
kDa
Macro
NK
CASPASE-1
CASPASE-4
GBP1
GBP2
GBP5
αTUBULIN
H3
52
66
16
*1
*2

841

Figure 2

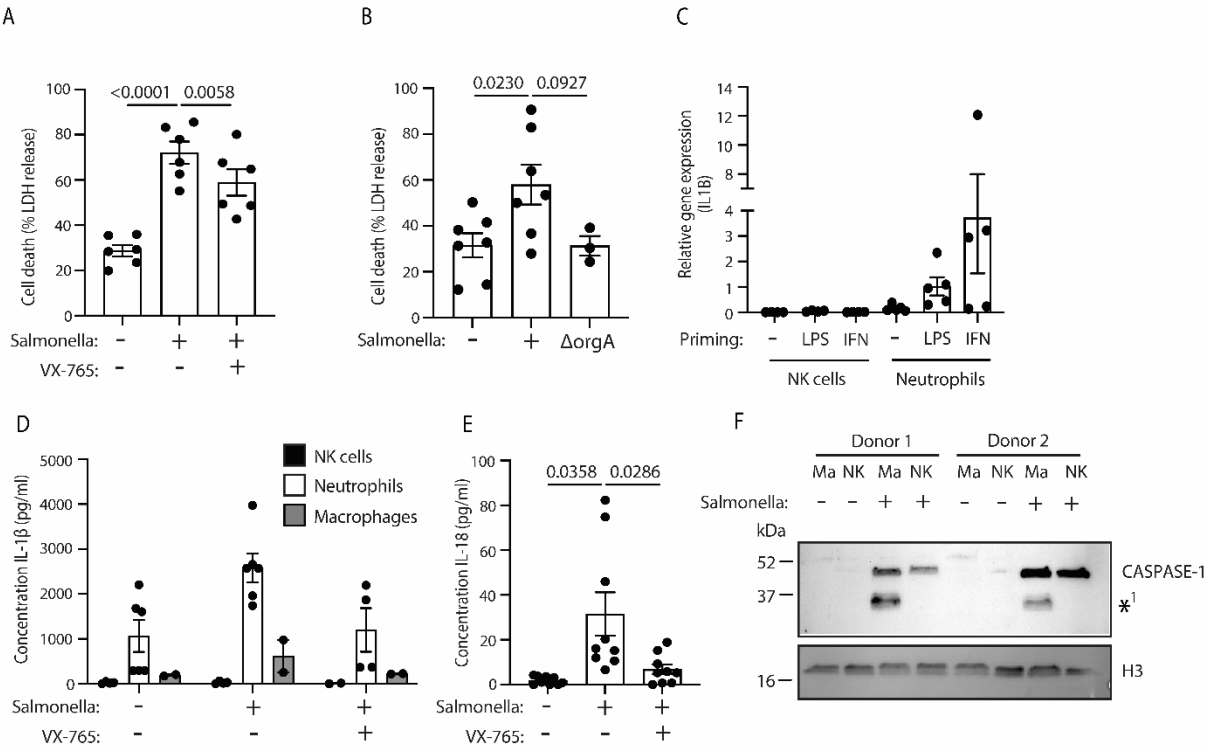
A
<0.0001
0.0058
Cell death (% LDH release)
Salmonella:
VX-765:
B
0.0230
0.0927
Cell death (% LDH release)
Salmonella:
ΔorgA
C
Relative gene expression (IL1B)
Priming:
LPS
IFN
NK cells
Neutrophils
D
NK cells
Neutrophils
Macrophages
Concentration IL-1β (pg/ml)
Salmonella:
VX-765:
E
0.0358
0.0286
Concentration IL-18 (pg/ml)
Salmonella:
VX-765:
F
Donor 1
Donor 2
Ma NK Ma NK Ma NK Ma NK
Salmonella:
kDa
52
37
16
CASPASE-1
*1
H3

842

Figure 3

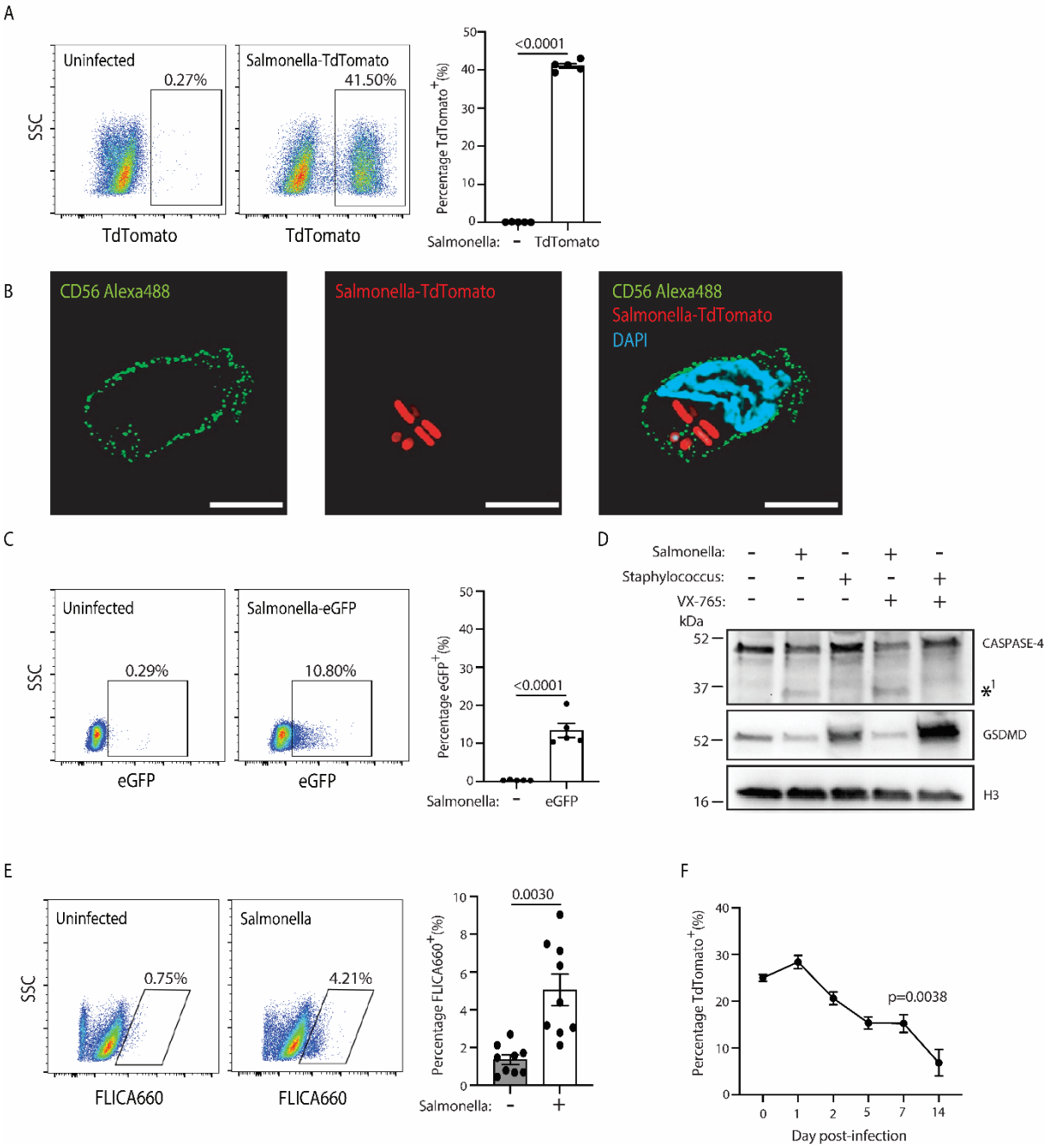
A
Uninfected
0.27%
Salmonella-TdTomato
41.50%
SSC
TdTomato
TdTomato
<0.0001
Percentage TdTomato+ (%)
Salmonella: - TdTomato
B
CD56 Alexa488
Salmonella-TdTomato
CD56 Alexa488
Salmonella-TdTomato
DAPI
C
Uninfected
0.29%
Salmonella-eGFP
10.80%
SSC
eGFP
eGFP
<0.0001
Percentage eGFP+ (%)
Salmonella: - eGFP
D
Salmonella: - + - + -
Staphylococcus: - - + - +
VX-765: - - - + +
kDa
52
37
52
16
CASPASE-4
*1
GSDMD
H3
E
Uninfected
0.75%
Salmonella
4.21%
SSC
FLICA660
FLICA660
0.0030
Percentage FLICA660+ (%)
Salmonella: - +
F
Percentage TdTomato+ (%)
p=0.0038
0 1 2 5 7 14
Day post-infection

843

Figure 4

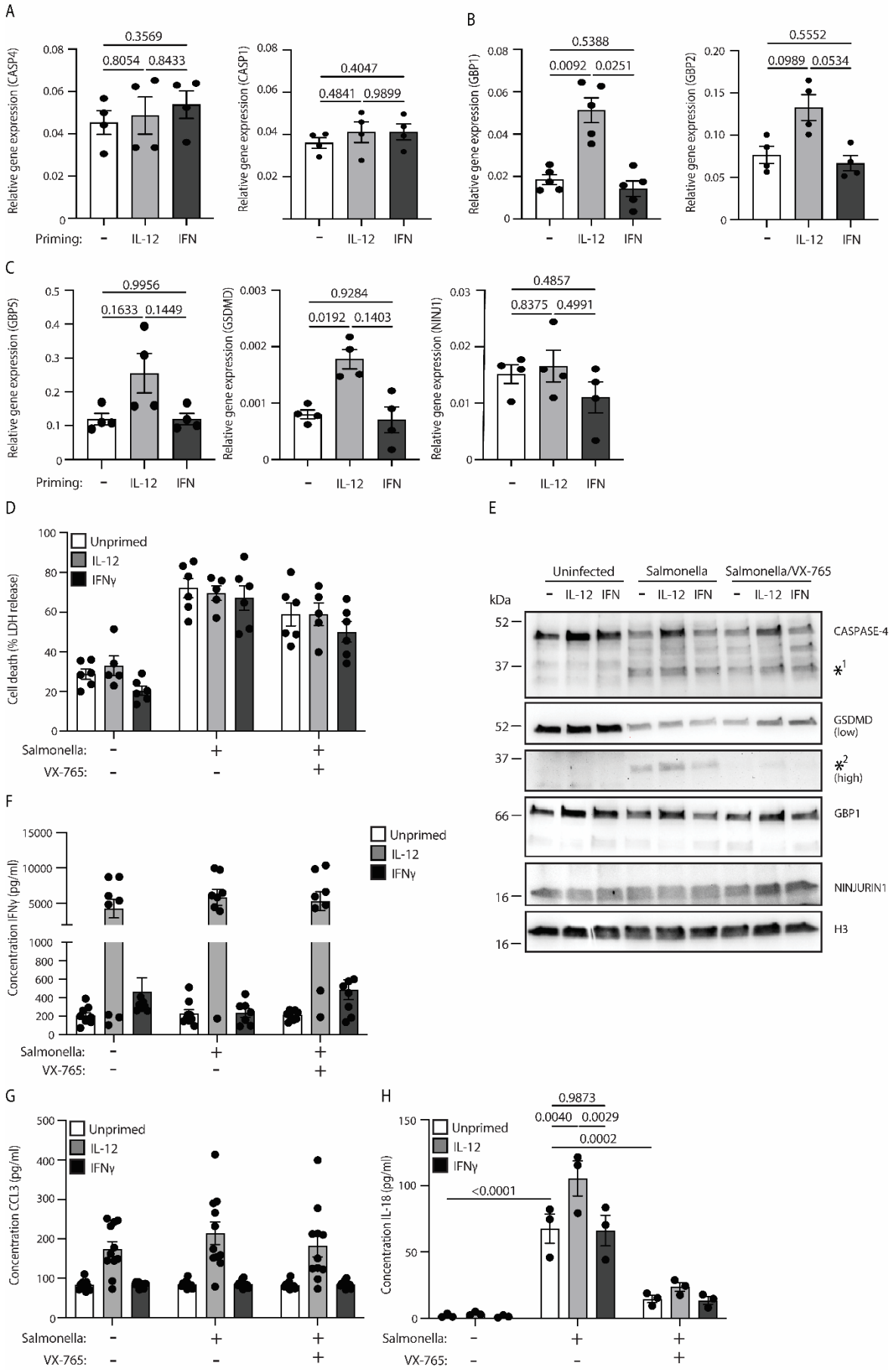
A
Relative gene expression (CASP4)
0.3569
0.8054 0.8433
Relative gene expression (CASP1)
0.4047
0.4841 0.9899
Priming: - IL-12 IFN
B
Relative gene expression (GBP1)
0.5388
0.0092 0.0251
Relative gene expression (GBP2)
0.5552
0.0989 0.0534
C
Relative gene expression (GBP5)
0.9956
0.1633 0.1449
Relative gene expression (GSDMD)
0.9284
0.0192 0.1403
Relative gene expression (NINJ1)
0.4857
0.8375 0.4991
D
Unprimed
IL-12
IFNγ
Cell death (% LDH release)
Salmonella:
VX-765:
E
Uninfected
Salmonella
Salmonella/VX-765
kDa
CASPASE-4
GSDMD (low)
(high)
GBP1
NINJURIN1
H3
F
Concentration IFNγ (pg/ml)
G
Concentration CCL3 (pg/ml)
H
Concentration IL-18 (pg/ml)
0.9873
0.0040 0.0029
0.0002
<0.0001

844

Supplementary Table 1

A

Human gene	Taqman ID
NLRP3	Hs00918062
NLRC4	Hs00892666
NINJ1	Hs00982607
TLR4	Hs00152939
GSDMD	Hs00226875
Casp1	Hs003354836
Casp4	Hs01031951
Casp5	Hs07290189
GBP1	Hs00266717
GBP2	Hs00894837
GBP5	Hs00369472
GzmA	Hs009869184
IFNGR1	Hs00166223
GAPDH	Hs02758991
IL1B	Hs01555410

Mouse gene	Taqman ID
Ninj1	Mm00479014
Gsdmd	Mm00509958
Il1a	Mm00439620
Il1b	Mm00434228
Il118	Mm00434225
Gbp2b	Mm00657086
Gbp5	Mm00463735
Ifngr1	Mm00599890
Cd14	Mm00438094
Tlr4	Mm00445273
Casp1	Mm00438023
Casp4	Mm00432304
Pycard	Mm00445747

B

Human antibody target	Clone number	Catalog number	Supplier	Use
CASPASE-1	D7F10	3866	Cell Signalling	WB
GBP1	polyclonal	15303-1-AP	Proteintech	WB
GBP2	polyclonal	11854-1-AP	Proteintech	WB
GBP5	polyclonal	13220-1-AP	Proteintech	WB
αTubulin	1E4C11	66031-1-Ig	Proteintech	WB
CASPASE-4	1D1E12	67398-1-Ig	Proteintech	WB
GAPDH	1E6D9	60004-1-Ig	Proteintech	WB
NINJURIN 1	2G5	H00004814-MO1A	Abnova	WB
GSDMD	E9S1X	39754S	Cell Signalling	WB
NLRP1	9F9B12	679802	Biolegend	WB
H3	1A2A3	68345-1-Ig	Proteintech	WB
CD45 BUV395	HI30	363-0459-42	Thermo	FC
CD4 PE	SK3	60122PE	StemCell Technologies	FC
CD8a PE	HIT8a	300908	Biolegend	FC
CD19 PE	HIB19	302208	Biolegend	FC
CD14 PE	HCD14	325605	Biolegend	FC
CD123 PE	6H6	306006	Biolegend	FC
CD303 PE	201A	354204	Biolegend	FC
CD3e BV605	UCHT1	300459	Biolegend	FC
CD16 BV480	eBioCB16	414-0168-41	Thermo	FC
CD56 BUV661	TULY56	376-0566-42	Thermo	FC
CD127 PECy7	R34.34	25-1271-82	Thermo	FC
CD2 AlexaFluor700	RPA-2.10	300238	Biolegend	FC
CD57 BV421	QA17.A04	393326	Biolegend	FC
NCAM1 (CD56)	E7X9M	99746	Cell Signalling	IF
Mouse antibody target	**Clone Number**	**Catalog Number**	**Supplier**	**Use**
Caspase-11	17D9	NB120-10454	Novus Biologicals	WB
GBP2	polyclonal	11854-1-AP	Proteintech	WB
H3	1A2A3	68345-1-Ig	Proteintech	WB
CD45 AlexaFluor700	30-F11	103128	Biolegend	FC
CD3 PE	17A2	100206	Biolegend	FC
CD4 PE-Cy7	GK1.5	100421	Biolegend	FC
CD8a PE-Cy7	53-6.7	100721	BioLegend	FC
CD19 PE-Cy7	1D3	25-0193-82	eBioscience	FC
CD11b BV510	M1/70	101263	Biolegend	FC
CD11c PE-Cy7	N418	117317	BioLegend	FC
FceR1a PE-Cy7	MAR-1	134317	BioLegend	FC
Gr1 PE-Cy7	RB6-8C5	108416	BioLegend	FC
NK1.1 BV421	PK136	108732	Biolegend	FC
Other antibodies	**Clone Number**	**Catalog Number**	**Supplier**	**Use**
Mouse Ig-HRP	Polyclonal	RGAM001	Proteintech	WB
Rabbit Ig-HRP	Polyclonal	RGAR001	Proteintech	WB
Anti-rabbit IgG (H+L), (Alexa Fluor® 488 Conjugate)	F(ab')2 Fragment	4412	Cell Signalling	IF

845

Supplementary Figure 1

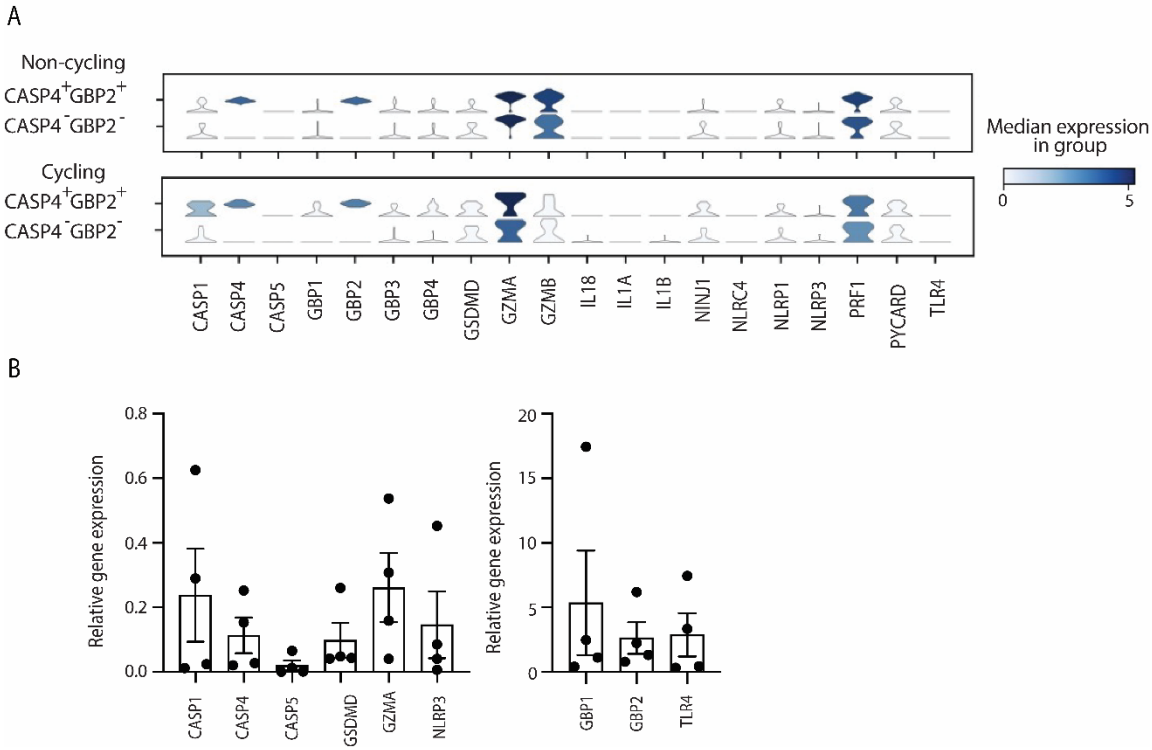

Supplementary Figure 2

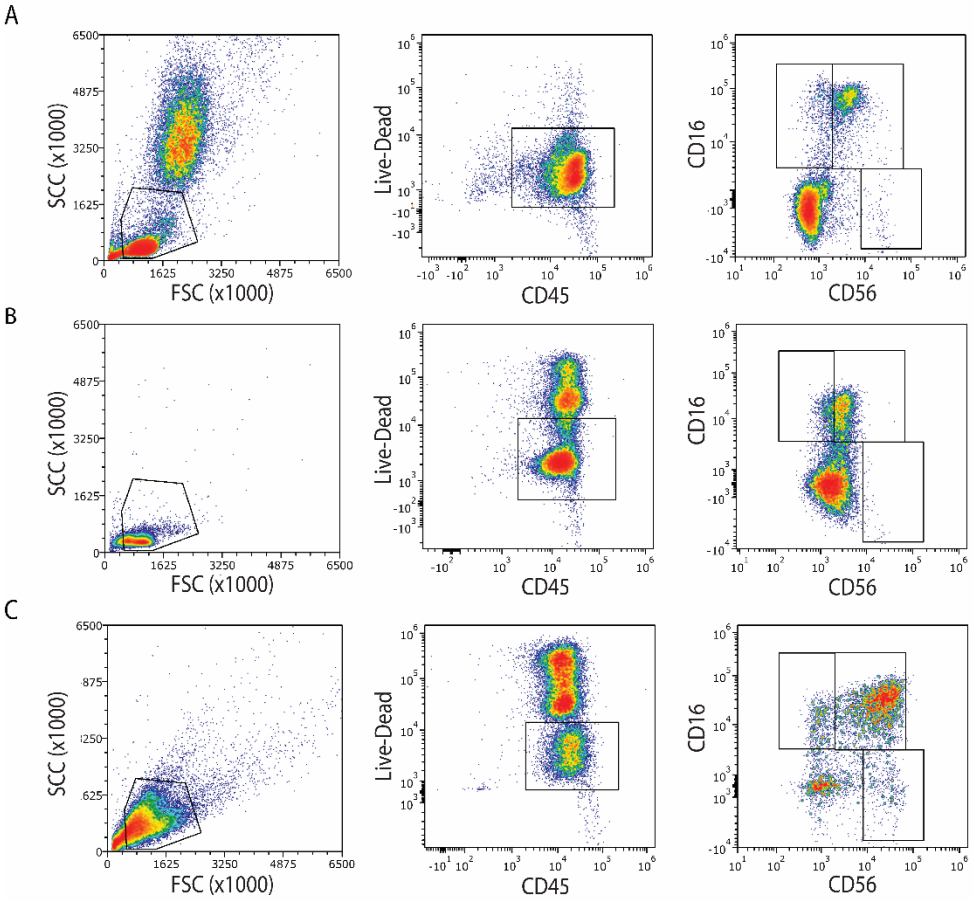

849

Supplementary Figure 3

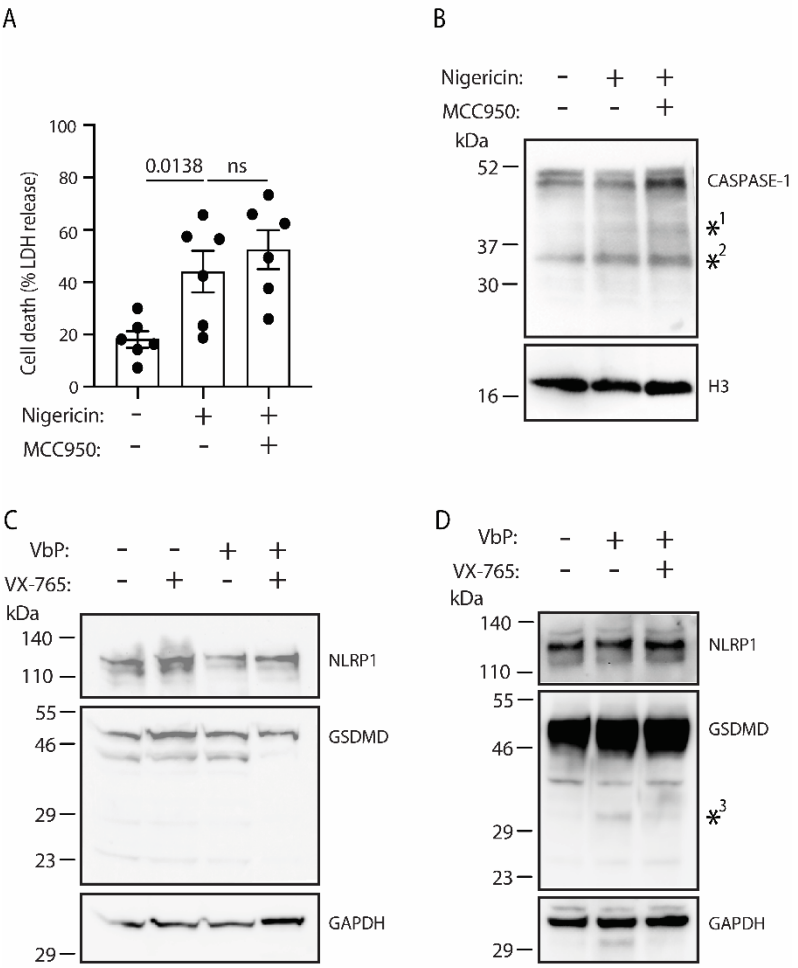

850

Supplementary Figure 4

A

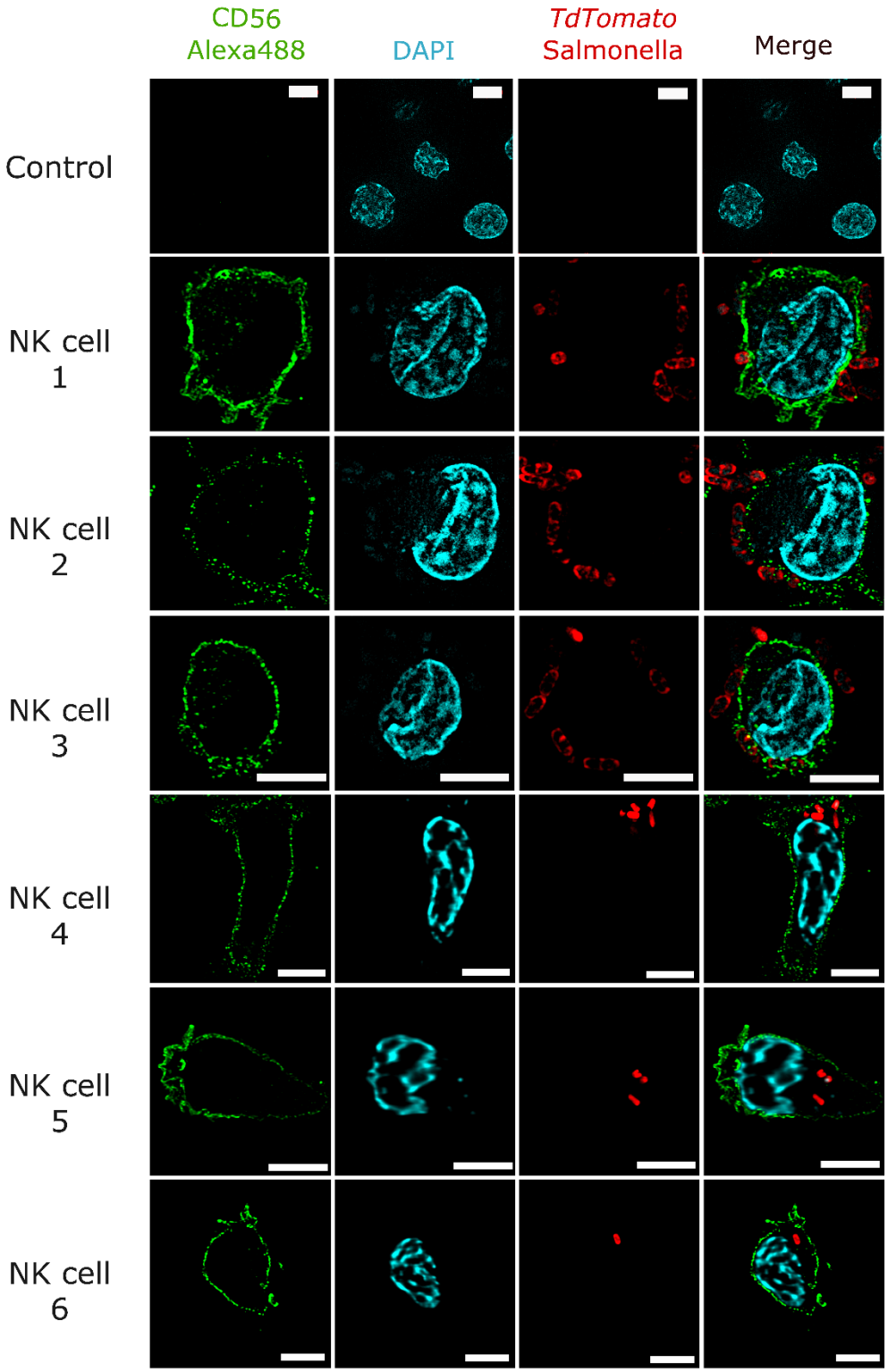

B

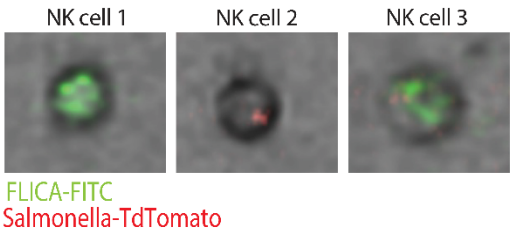

Supplementary Figure 5

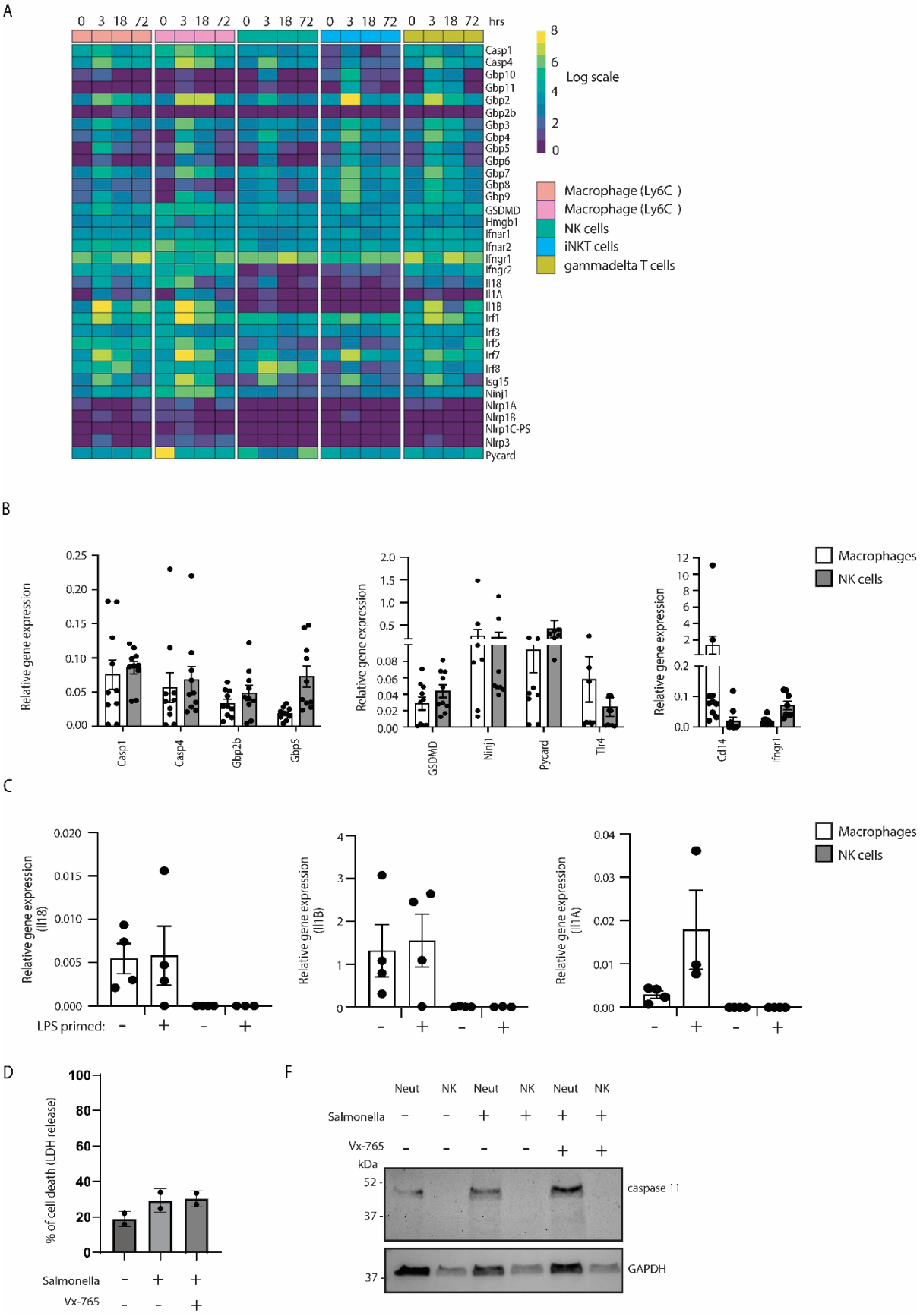

852